Article

Cell Reports

The Directional Response of Chemotactic Cells Depends on a Balance between Cytoskeletal Architecture and the External Gradient

Graphical Abstract

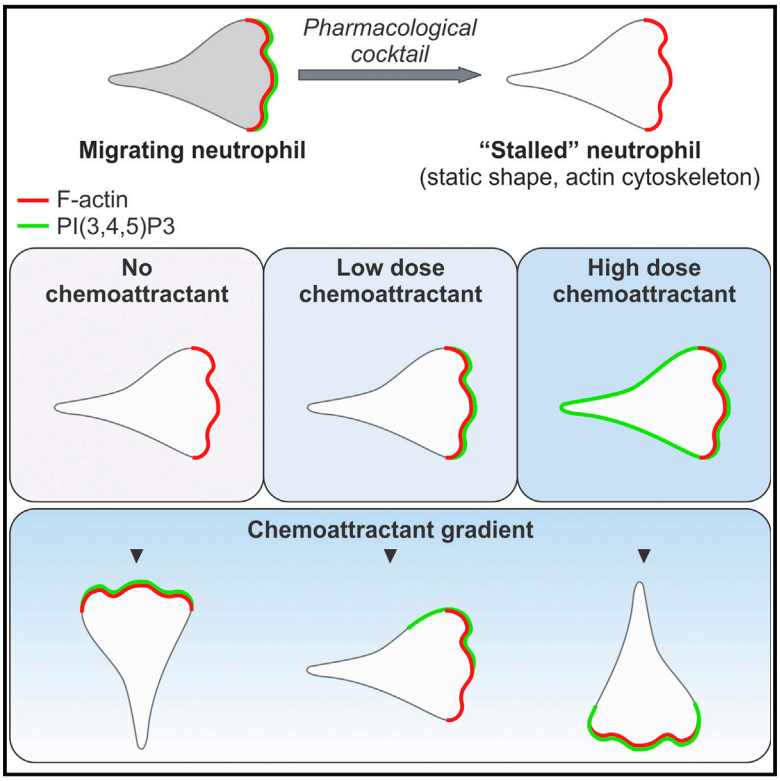

Highlights

Polarized sensitivity to chemoattractants is independent of cytoskeletal dynamics

Threshold for response is correlated with static F-actin distribution

Immobilized cells retain characteristic responses to spatial and temporal stimuli

Overall directional response depends on gradient and internal polarity

Authors

Ming-Jie Wang, Yulia Artemenko, ..., Pablo A. Iglesias, Peter N. Devreotes

Correspondence

pnd@jhmi.edu

In Brief

Wang et al. report that polarized sensitivity, a process of fundamental importance in neutrophil function, does not require cell movement and actin dynamics. They demonstrate that although direction sensing can exist without feedback from dynamic cell migration, it is biased by the static F-actin distribution, which is related to internal polarity.

Wang et al., 2014, Cell Reports 9, 1110–1121
November 6, 2014 ©2014 The Authors
http://dx.doi.org/10.1016/j.celrep.2014.09.047

OPEN ACCESS
CellPress

Cell Reports
Article

The Directional Response of Chemotactic Cells Depends on a Balance between Cytoskeletal Architecture and the External Gradient

Ming-Jie Wang,[1,2] Yulia Artemenko,[1] Wen-Jie Cai,[1,3] Pablo A. Iglesias,[1,4] and Peter N. Devreotes[1,*]
[1]Department of Cell Biology, Johns Hopkins University School of Medicine, Baltimore, MD 21205, USA
[2]Department of Physiology and Pathophysiology, Fudan University Shanghai Medical College, Shanghai 200032, China
[3]Department of Basic Medicine, University of Shanghai for Science and Technology, Shanghai 200093, China
[4]Department of Electrical and Computer Engineering, Johns Hopkins University, Baltimore, MD 21218, USA
*Correspondence: pnd@jhmi.edu
http://dx.doi.org/10.1016/j.celrep.2014.09.047

SUMMARY

Polarized migrating cells display signal transduction events, such as activation of phosphatidylinositol 3-kinase (PI3K) and Scar/Wave, and respond more readily to chemotactic stimuli at the leading edge. We sought to determine the basis of this polarized sensitivity. Inhibiting actin polymerization leads to uniform sensitivity. However, when human neutrophils were "stalled" by simultaneously blocking actin and myosin dynamics, they maintained the gradient of responsiveness to chemoattractant and also displayed noise-driven PIP_3 flashes on the basal membrane, localized toward the front. Thus, polarized sensitivity does not require migration or cytoskeletal dynamics. The threshold for response is correlated with the static F-actin distribution, but not cell shape or volume changes, membrane fluidity, or the preexisting distribution of PI3K. The kinetics of responses to temporal and spatial stimuli were consistent with the local excitation global inhibition model, but the overall direction of the response was biased by the internal axis of polarity.

INTRODUCTION

Directed cell migration is a fundamental cell biological process that plays an important role in embryogenesis and wiring of the nervous system, immune cell trafficking, wound healing, and a host of other critical physiological events. It also contributes to the pathogenesis of inflammatory diseases and cancer metastasis. Neutrophils exhibit a robust chemotactic response to chemical gradients and serve as a model for understanding this process. The similarity in the behavior of neutrophils to that of simple amoeboid cells, such as *Dictyostelium*, indicates that chemotaxis is a highly conserved fundamental cell biological process.

The mechanisms cells use to sense and migrate toward external cues are beginning to be elucidated. Directed migration depends on the seamless integration of motility, directional sensing, and polarity. Motility relies on spontaneous activation of signaling and cytoskeletal events and extension of pseudopods. Directional sensing is independent of the cytoskeleton, since external gradients can localize signaling activities in immobilized cells. Chemotactic cells are also often polarized, which increases the efficiency of the response.

Even without directional information, cells can establish an elongated polarized state with differential sensitivity between the front and the back. This cellular state is semistable and can be reset. Neutrophil-like HL-60 cells often make a "U-turn" rather than generate a new front when a chemoattractant is delivered by a micropipette toward the back of the cell (Gerisch and Keller, 1981). Elongated *Dictyostelium* cells, late in their developmental program, behave similarly when presented with a new gradient (Futrelle et al., 1982; Swanson and Taylor, 1982). Thus, when the gradient is shifted, polarized cells maintain their original direction and then gradually reorient toward the gradient. This suggests that cell polarity and gradient sensing might be separate, interacting phenomena. Although the established leading edge is relatively more sensitive to chemoattractants, cells can be forced to repolarize by increasing the steepness of the reverse gradient, indicating that some sensitivity is maintained around the entire perimeter. It is unclear what determines this dynamic "polarized sensitivity" and how it is related to gradient sensing.

It has been assumed that cell movement and cytoskeletal dynamics play a critical role in establishing and maintaining polarity. Most schemes for polarity couple positive feedback at the anterior with global inhibitory mechanisms to prevent additional fronts (Howell et al., 2009; Meinhardt, 1999; Neilson et al., 2011; Orchard et al., 2012). Recent models, for example, suggest that protrusions at the front alter membrane properties, such as membrane tension or curvature, which affects cytoskeletal activity at secondary sites (Frost et al., 2009; Houk et al., 2012). There is general agreement that pharmacological perturbations of F-actin abolish cell polarity (Casella et al., 1981; Spector et al., 1983). Signal transduction responses can still be elicited by chemoattractant in such immobilized cells, but the cells are equally sensitive around their perimeter. These observations support the belief that cytoskeletal dynamics and migration are essential for maintenance of the polarized state (Wang et al., 2002).

Studies with a pharmacological cocktail (JLY) containing actin disassembly inhibitor jasplakinolide (J), actin polymerization inhibitor latrunculin B (L), and ROCK inhibitor Y27632 (Y), which preserves the existing actin cytoskeleton while blocking assembly, disassembly, and rearrangement of the actin network, also suggest that cytoskeletal dynamics are important for aspects of polarity. JLY-treated HL-60 neutrophils stop migrating and maintain their shape, although Rac activity seen at the leading edge of moving cells disappears (Dandekar et al., 2013; Peng et al., 2011). Thus a dynamic cytoskeleton appears to be necessary to maintain polarization in the signal transduction system. However, polarized sensitivity to chemoattractants was not examined in these experiments.

By manipulating the polarity of HL-60 neutrophils and examining the responses of moving and immobilized cells to uniform increases and gradients of the chemoattractant, N-formyl-L-methionyl-L-leucyl-L-phenylalanine (fMLP), we were able to distinguish the contributions of motility, directional sensing, and polarity to the overall response. As previously shown for latrunculin-treated cells, we find that JLY-treated, ''stalled'' cells respond and adapt to uniform stimuli and respond persistently to applied gradients. Furthermore, we find that polarized sensitivity depends strongly on cytoskeletal architecture and does not depend on cell shape, volume, membrane curvature, or membrane fluidity. Thus, the overall directional response of the cell depends on the balance between the external gradient and the polarized architecture of the cytoskeleton. These conclusions are consistent with the turning behaviors of cells exposed to shifting gradients.

RESULTS

Responses to Chemoattractant and Spontaneous Activities Are Polarized in JLY-Treated, "Stalled" Neutrophils

We first compared the morphology and migration behavior of cells before and after JLY treatment. As previously reported, cells kept migrating in the presence of a ROCK inhibitor Y27632 but stopped as soon as latrunculin B and jasplakinolide were added (Peng et al., 2011; Xu et al., 2003). Cell shape, judged by phase microscopy, and actin cytoskeletal architecture examined by the F-actin biosensor, Lifeact, was maintained for at least 2 hr. We also verified that the rate of fluorescence recovery after photobleaching (FRAP) of actin-mCherry was negligible (see below). Latrunculin B treatment also immobilized cells, but the cell shape and cytoskeletal architecture was not maintained (Figure 1A) (Riedl et al., 2008). As observed in *Dictyostelium*, the PIP_3 biosensor pleckstrin homology domain of serine-threonine protein kinase AKT1 (PH-AKT), typically observed at the front of migrating cells, decreased following latrunculin B treatment (Figure S1A). Furthermore, PIP_3 rapidly decreased following JLY treatment of cells migrating in uniform fMLP (Figure S1A). This suggests that even the JLY-stabilized cytoskeleton cannot maintain activated phosphatidylinositol 3-kinase (PI3K).

Previous studies have suggested that there is feedback from actin polymerization to activation of PI3K, although the conclusions have been based principally on the ability of latrunculin B to block the process (Inoue and Meyer, 2008; Srinivasan et al., 2003; Wang et al., 2002). When we transiently photoactivated Rac in differentiated HL-60 cells expressing PH-AKT-GFP, we observed a 14.4% ± 1.5% increase in PIP_3 (Figure S1B). However, the increase was negligible in cells treated with JLY or latrunculin B plus nocodazole. These observations suggest that actin dynamics and/or movement are required for feedback regulation from Rac activation to PI3K activity in neutrophils.

Surprisingly, when we exposed the JLY-treated, stalled cells to a uniform, low concentration (1nM) of fMLP, not only did they generate PIP_3, but it was accumulated in a gradient (Figures 1B and 1C; Figure S1C; Movie S1). The levels were higher at the front and sides than the back, indicating that the anterior is more sensitive to PI3K activation. When we increased the global fMLP concentration (100 nM) applied to the same cell, there was no significant difference between back and front maximum membrane PH-AKT accumulation (Figure 1C). The same results were obtained whether cells were pretreated with JLY for several minutes or 2 hr. Cells with obviously polarized morphology were used for quantification (Figure S1E). Using the C5a receptor as a membrane marker, we verified that the graded signal was not due to an uneven membrane distribution from front to back (Figure S1A). In contrast to the JLY cells, rounded cells treated with nocodazole and latrunculin B responded equally along the entire membrane at all concentrations of fMLP (Figures 1B and 1C; Movie S2). The responses at the back of the JLY-treated cells peaked at a lower level and were briefer than those at the front and sides (Figure 1C; Figures S1C and S1D). Both the amplitude and duration contribute to a smaller integrated response seen at the back. PH-AKT translocated to a broader membrane region with increasing doses of fMLP (Figure 1D). Together, these observations suggest there is an anterior-posterior gradient of sensitivity for chemoattractant-mediated activation of PI3K and PIP_3 accumulation in the JLY-treated, stalled neutrophils.

Previous studies have shown that Hem1 is spontaneously recruited in waves to the basal surface of migrating neutrophils and accumulates at the edge of the basal surface in response to fMLP (Weiner et al., 2007). The spontaneous waves are silenced by latrunculin. Similarly, we found that Hem1 waves disappeared in JLY-treated cells. Although JLY-treated cells were less sensitive than untreated cells, Hem1 was recruited transiently to the boundary of the basal membrane after stimulation with 100 nM fMLP, and the response was more persistent at the front than at the back (Figure 1E), as was the case for PIP_3 production (Figure S1D).

Recent studies showing there are independent excitable signal transduction and oscillatory cytoskeletal networks in *Dictyostelium* cells and the fact that cytoskeletal component Hem-1 displays propagating waves in neutrophils (Huang et al., 2013; Weiner et al., 2007) prompted us to further explore the similarities in the chemotactic systems in the two cell types. To ask whether there are similar separable networks in neutrophils, we monitored by total internal reflection fluorescence (TIRF) microscopy the spontaneous recruitment of PH-AKT to the membrane on the basal surface of randomly migrating or stalled JLY-treated neutrophils. We observed spontaneously appearing PIP_3 patches with a lifetime of a few minutes in the majority of randomly migrating cells. T-stacks (Huang et al., 2013) of coexpressed PH-AKT and Lifeact showed the two overlapped

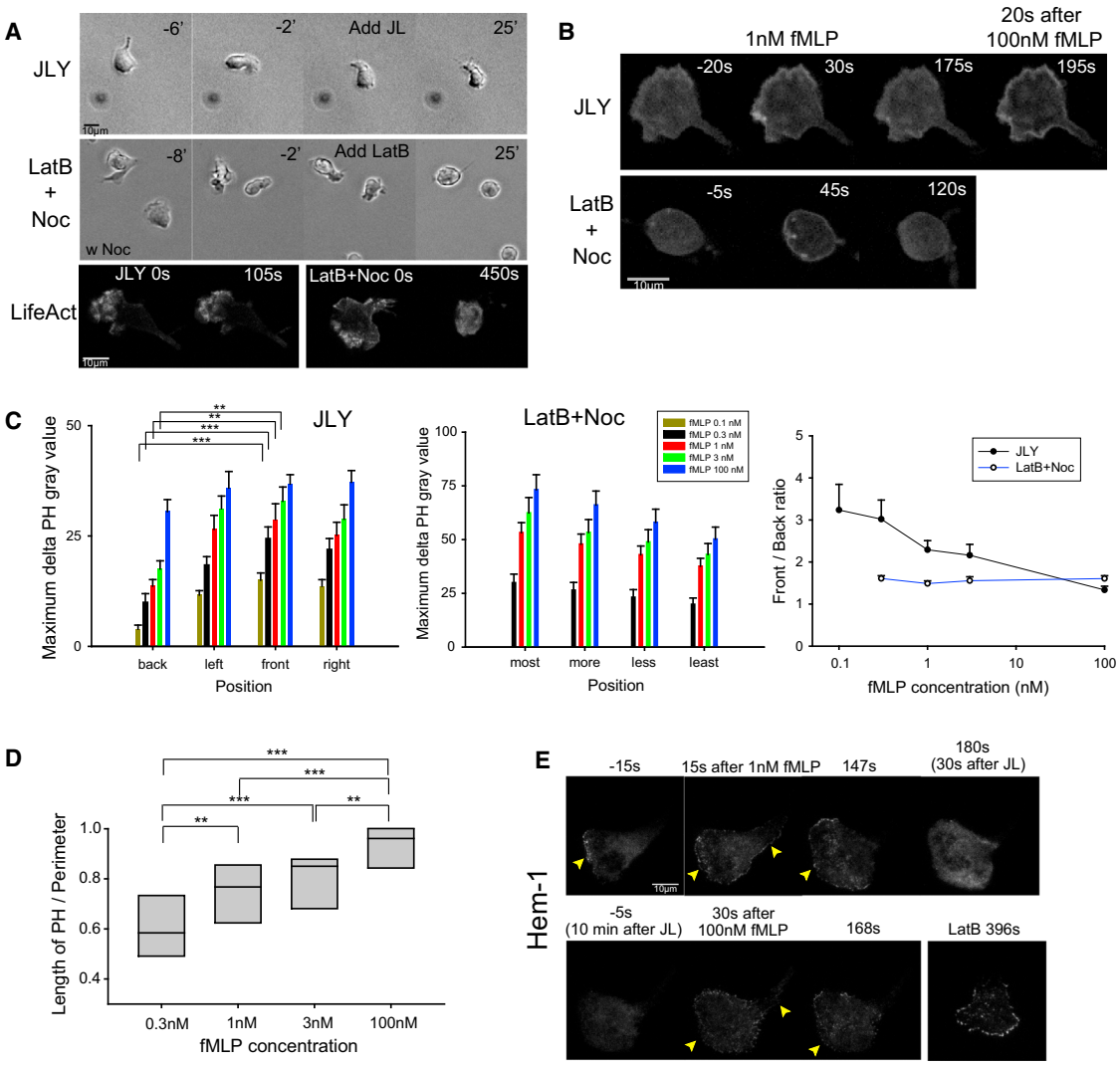

Figure 1. Response to Chemoattractant in Stalled Neutrophils

(A) Phase images of JLY or latrunculin B + nocodazole-treated cells. Lifeact localization before and after drug treatment. Scale bar, 10 μm.

(B) Fluorescence images of PIP_3 production with uniform fMLP stimulation using PH-AKT-GFP expressing HL-60 neutrophils treated with JLY or latrunculin B + nocodazole. Scale bar, 10 μm. See also Movies S1 and S2.

(C) Quantification of PIP_3 production with different doses of global fMLP in JLY or latrunculin B + nocodazole-treated neutrophils. Left panel is peak responses to different concentrations of fMLP along the perimeter of JLY-treated cells normalized to the expression level. The differences between back and front peak response to 0.1, 0.3, 1, and 3 nM fMLP are significant (**$p < 0.01$; ***$p < 0.001$). n = 14 for 0.1 nM fMLP, n = 19 for 0.3 nM fMLP, n = 25 for 1 nM fMLP, n = 20 for 3 nM fMLP, and n = 24 for 100 nM fMLP. Error bars represent SEM. Middle panel is "positioned quantification" for latrunculin B + nocodazole cells. The position is ranked by most, more, less, or least maximum delta PH-AKT gray value within 30 s after stimulation. There is no significant difference between groups. n = 30 for 0.3 nM fMLP, n = 22 for 1 nM fMLP, n = 21 for 3 nM fMLP, and n = 27 for 100 nM fMLP. Error bars represent SEM. Right panel is the relationship between ratio of "front/back" (for JLY) or "most/least" (for latrunculin B + nocodazole) maximum delta PH gray value and increasing fMLP concentration. See also Figure S1.

(D) Dose summary of responsive membrane fraction in JLY-treated neutrophils. The box plot shows the median, 25th, and 75th percentiles. n = 19 for 0.3 nM fMLP, n = 25 for 1 nM fMLP, n = 20 for 3 nM fMLP, and n = 24 for 100 nM fMLP. **: $p < 0.01$; ***: $p < 0.001$.

(E) TIRF image of Hem1-YFP in JLY-treated neutrophils. Arrowheads point to Hem1 recruited to the boundary of the basal membrane. Cells in Y were exposed to 1 nM fMLP, then treated with JL, and then stimulated with 100 nM fMLP as indicated. On the right, latrunculin B-treated cells are shown for comparison. Scale bar, 10 μm.

but were not precisely colocalized (Figure S1F; Movie S3). Interestingly, we observed similar dynamic PIP_3 patches in JLY-treated cells; however, unlike in randomly migrating cells, the F-actin signal was static (Figure 2A). There was more PIP_3 activity at the anterior of the cell, where static F-actin was enriched, than at the back (68.1% versus 31.9% of total intensity of PIP_3 fluctuations, $p < 0.001$, n = 7) (Figure 2A; Movie S4). Coexpressed membrane marker C5aR showed that the PH-AKT flashes were not due to membrane deformations or rearrangements (Figure 2B; Movie S5). The addition of 20 μM PI3Kγ

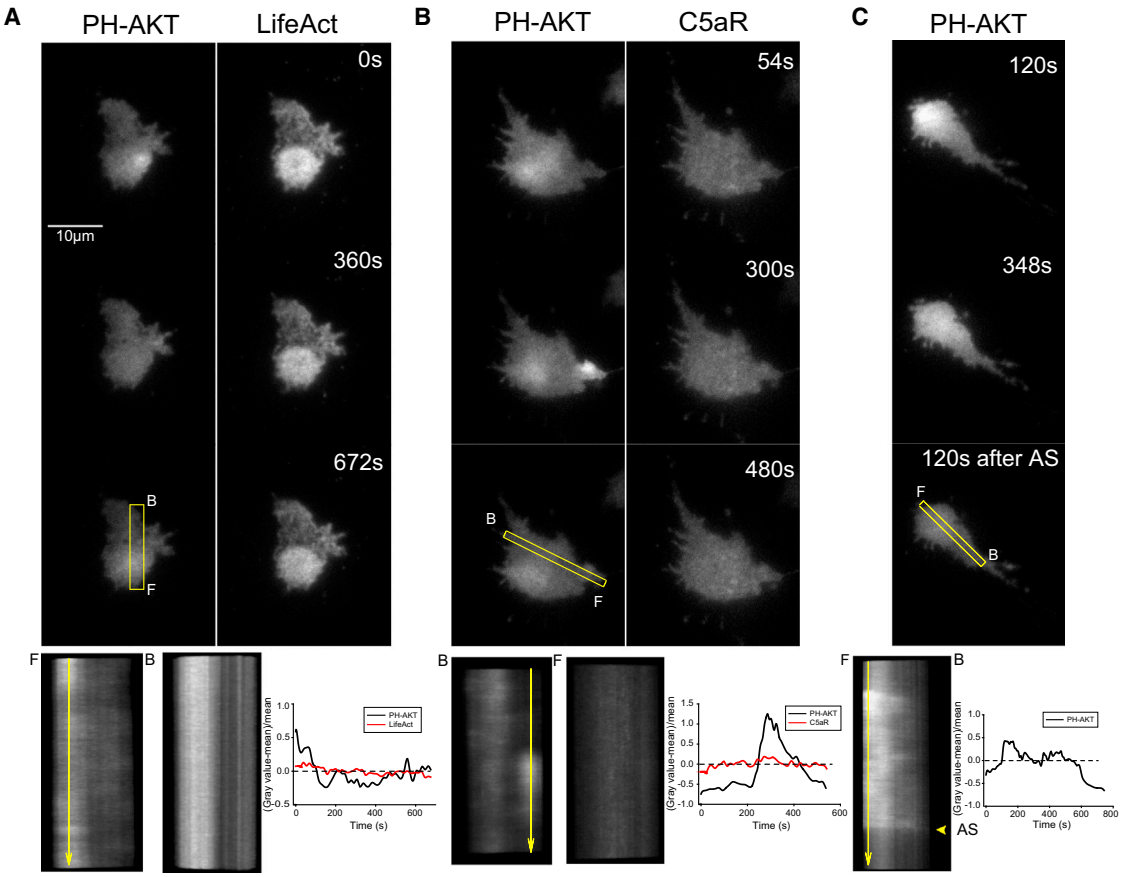

Figure 2. TIRF Images of Spontaneous Recruitment of PH-AKT to the Membrane on the Basal Surface of JLY-Treated Neutrophils

(A) Dual-view TIRF images of coexpressed PH-AKT and Lifeact signals in JLY-treated neutrophils. T-stacks of both panels in the same cross-section show the signal dynamics. Vertical line scans at the point indicated by the yellow arrows are used to highlight dynamic changes in gray value over time. Detailed description of vertical line scans is described in Supplemental Experimental Procedures. See also Movie S4.

(B) Dual-view TIRF images of coexpressed PH-AKT and C5aR signals in JLY-treated neutrophils. T-stacks and vertical line scans of both panels are also shown. See also Movie S5.

(C) TIRF images of PH-AKT in JLY-treated neutrophils treated with PI3K inhibitor AS605240. T-stack and a vertical line scan are also shown.

inhibitor AS605240 abolished the PH-AKT flashes (Figure 2C). Taken together, these observations show the chemotactic signal transduction network in neutrophils displays spontaneous activity in the absence of cytoskeletal activity or movement and, furthermore, that the activity is biased toward the front.

Polarized Sensitivity Is Correlated with the Arrested F-actin Distribution and Is Independent of Cell Shape, Volume, Membrane Curvature, or Fluidity

Since polarized migrating neutrophils usually have more F-actin at the front (Nishikimi et al., 2009), we speculated that the polarized sensitivity might be related to the arrested F-actin distribution. Examples of cells with broader or narrower Lifeact regions appear to support this (Figure 3A). Quantification showed that when exposed to a uniform, low concentration of fMLP, JLY-treated cells with narrower regions of F-actin, as indicated by a higher ratio of Lifeact fluorescence intensity at the front versus the back, also had narrower zones of PIP_3 production on the membrane. The asymmetric response was nearly absent when we increased the fMLP concentration applied to the same cell (Figure 3A; Movies S6 and S7).

We assessed several other factors that could potentially underlie the polarized sensitivity of the JLY-treated cells. First, there is a marked difference in shape and curvature between fan-like fronts and elongated backs. Since polarized HL-60 neutrophils with broad backs were rare, we artificially produced wide tails in polarized cells by exposing JLY-treated cells to hypotonic buffer. At room temperature, the increased volume caused by hypotonic treatment lasts for at least 25 min (Ting-Beall et al., 1993). In our experiments, some of the JLY-treated cells that had loosely attached backs formed large rounded backs that had even less curvature than the front. When we exposed these cells to low fMLP, they still did not respond at the back. The rounded backs did respond to higher concentrations of fMLP (Figure 3B). Thus, the polarized sensitivity was independent of cell shape, volume, or membrane curvature.

Interestingly, in some of the JLY-treated cells that appeared to adhere strongly to the substrate at the rear, hypotonic treatment

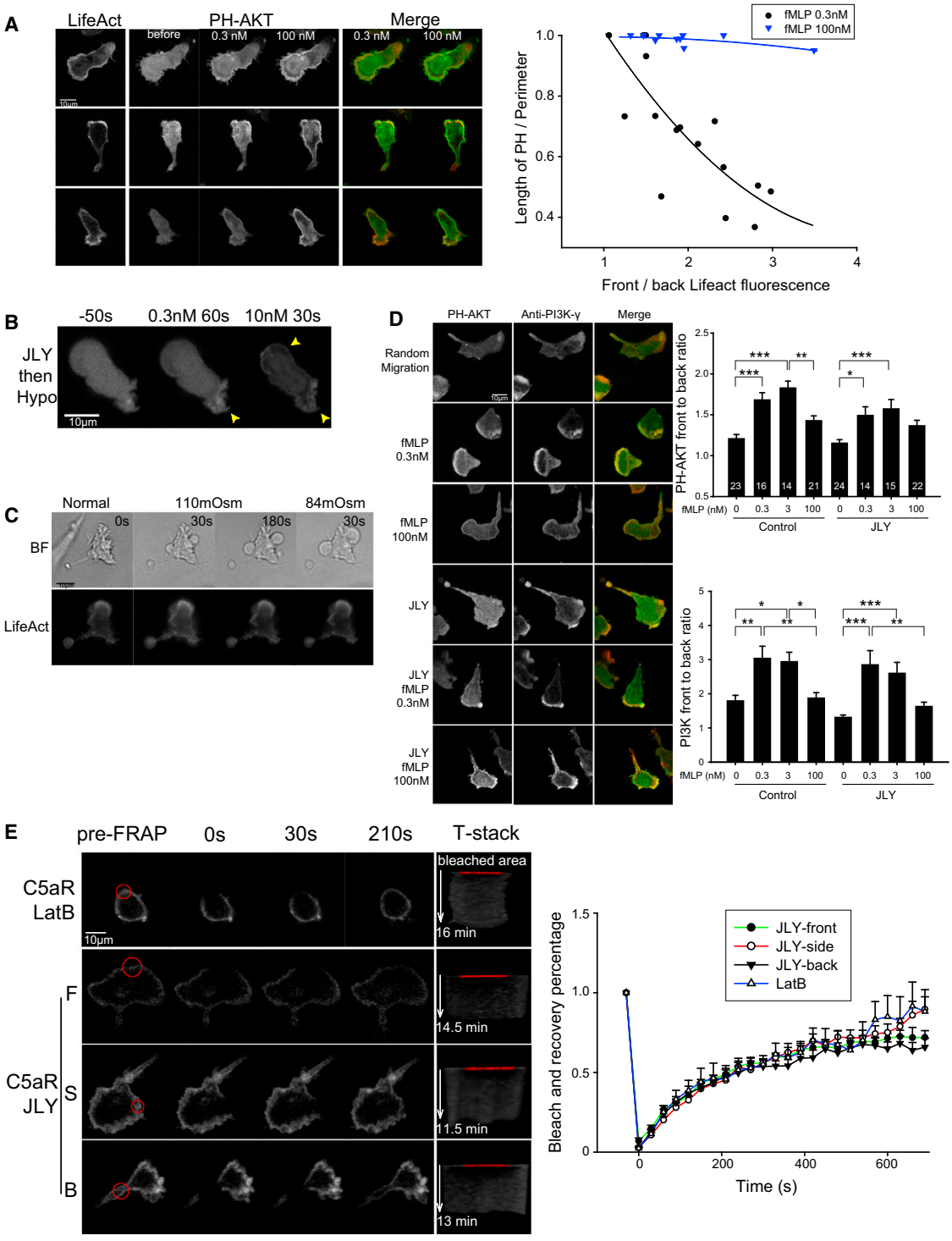

Figure 3. Polarized Sensitivity Is Correlated with the Arrested F-actin Distribution and Is Independent of Other Factors

(A) Fluorescence images of coexpressed PH-AKT and Lifeact signals in JLY-treated neutrophils exposed to uniform fMLP. The upper two panels or lower panel show cells with asymmetric or uniform Lifeact distributions, respectively. Merged images show the extent of co-localization. Graph on the right shows the relationship between length of PH-AKT as a fraction of the perimeter and front to back Lifeact fluorescence ratio. Trend lines (second degree polynomial) are also shown. Scale bar, 10 μm. See also Movies S6 and S7.

(B) Fluorescence images of PH-AKT in neutrophils treated with JLY for 10 min followed by 1:3 volume of hypotonic buffer for 20 min. Cells were exposed to uniform fMLP. The arrowheads indicate PIP_3 accumulation after fMLP stimulation. Scale bar, 10 μm.

(legend continued on next page)

did not produce a rounded back but instead induced blebs from the sides in the zone where the F-actin content dramatically decreased (32 out of 52 cells form side blebs; Figure 3C). This observation suggested that the membrane was more loosely attached to the cortex at the sides and that polarized sensitivity therefore cannot be traced to a differential attachment of the membrane to the cortex. Curiously, these blebs formed in hypotonic conditions retracted spontaneously or after adding fMLP (Figure S2A).

PI3K is found at the leading edge of chemotaxing *Dictyostelium* cells and several types of leukocytes (Funamoto et al., 2002; Gómez-Moutón et al., 2004), and if it were trapped at the fronts of the immobilized neutrophils by the JLY-treatment, the fronts would be expected to produce more PIP_3 in response to uniform stimuli. Using PI3Kγ catalytic subunit antibody staining, we verified that the enzyme was colocalized with PH-AKT at the leading edge in fMLP-treated, migrating HL-60 cells. However, we found that in the JLY-treated cells, PI3Kγ was not localized at the fronts before stimulus addition. Statistical analysis showed that PI3Kγ translocated selectively to the membrane at the front of JLY-treated neutrophils after exposure to uniform low fMLP, while a high fMLP caused a broader translocation of this enzyme (Figure 3D). These observations indicate that the polarized accumulation of PIP3 in JLY-treated cells is due to specific recruitment of PI3Kγ to the front.

Although the cytoskeleton is static in JLY-treated cells, the membrane may remain fluid. We used FRAP assays to assess components that reflect membrane fluidity. As noted above, actin dynamics were stalled in the JLY-treated cells, as there was no recovery of actin-mCherry fluorescence within 12 min after photobleaching (Figure S2B). By contrast, Lifeact red fluorescent protein (RFP) fluorescence recovered quickly, presumably since it exchanged rapidly on the F-actin (Figure S2B). Similarly, the PH-AKT signal recovered 90% within 2 min. The C5aR signal recovered more slowly (50% within 3 min), and the recovery came from adjacent membrane, not the cytosol. Importantly, there was no significant difference in C5aR mobility in JLY- versus latrunculin B-treated cells, and furthermore, no positional difference was found in stalled neutrophils (Figure 3E). Thus, differences in membrane fluidity do not appear to contribute to polarized sensitivity.

The Stimulus-Response Behavior of the Chemotactic System in Immobilized Cells

Previous studies have suggested that, like PI3K, Ras is activated by chemoattractants in neutrophils, although the localization of the activated form was not determined (Zheng et al., 1997). To extend these studies, we stimulated cells with fMLP and measured activation of K Ras and N Ras using pull-down assays with subtype-specific antibodies. We found that both subtypes were transiently activated upon fMLP stimulation, peaking around 30 s to 1 min (Figure S2C). We then expressed a fragment of Raf-1 containing the Ras binding domain plus the cysteine-rich domain (Raf-$1_{151–220}$-GFP) to study Ras activation in living cells. Raf-$1_{151–220}$-GFP translocated to the membrane after 100 nM fMLP stimulation and then accumulated at the leading edge during migration (Figure S2D). Using this more sensitive biosensor, we observed responses to fMLP in 75% of the cells that were studied (33 out of 44 cells). The sites of Ras activation and PIP_3 accumulation closely coincided, indicating that the polarized sensitivity we have described may involve multiple components of the signal transduction network (Figure S2E).

Differences in the responses of control and JLY-treated neutrophils to chemoattractant allowed us to separate the direct effects of the stimulus from those due to feedback from movement and/or cytoskeletal dynamics. As noted above, a uniform increase in chemoattractant elicits a transient activation of Ras or PI3K, but when the cells "break symmetry" and migrate, they display persistent PIP_3 at the leading edges (Servant et al., 2000). Unlike in migrating cells, the transient activations of PI3K and Ras triggered by uniform increases of fMLP in JLY-treated cells were not followed by persistent activity at the leading edge (Figures 4A and 4D; Figures S1D and S2F). Thus, the response to chemoattractant adapts during continuous uniform stimulation and the persistent response observed at the front of migrating cells depends on feedback from movement and/or cytoskeletal dynamics.

However, when JLY-treated neutrophils were exposed to a gradient of chemoattractant, the initial response was followed by a continuous steady-state response directed toward the high side. As shown in Figures 4A and 4B, when an fMLP-filled micropipette was placed in front of an immobilized cell, PH-AKT first translocated to the cell membrane, then formed a stable "crescent" facing more or less toward the tip. When the pipette was lifted, ending the stimulation, the PH-AKT crescent disappeared. Furthermore, the steady-state response toward gradient lasted as long as the gradient was present and disappeared rapidly when the stimulus was removed. The longest time tested was 30 min (Figures 4C and 4D; Movie S8). Comparison of the kinetics of the responses to 30 min uniform or gradient stimuli clearly showed that the former was transient, whereas the latter was persistent. Thus, as previously reported for responses of latrunculin-treated *Dictyostelium* cells (Parent et al., 1998), exposure of neutrophils to a gradient appears to bypass the adaptation process.

Polarity and Gradient Sensing Are Separable, Integrated Phenomena

To assess the effects of polarity on the directional response to a gradient, we compared polarized and unpolarized immobilized

(C) Phase and fluorescence images of Lifeact-expressing JLY-treated neutrophils exposed to sequential buffers of decreasing osmolarity as indicated. The times after each decrease are indicated. The duration of each treatment is approximately 5 min. Scale bar, 10 μm.

(D) Immunofluorescent staining of the catalytic subunit of PI3Kγ in randomly migrating and JLY-treated neutrophils expressing PH-AKT with or without fMLP stimulation. Scale bar, 10 μm. Bar graphs show the front to back ratio of PH-AKT and PI3Kγ. Numbers in the bars show the number of cells quantified. *$p < 0.05$; **$p < 0.01$; ***$p < 0.001$. Error bars represent SEM.

(E) C5aR fluorescent images before and after the FRAP assay in latrunculin B- and JLY-treated neutrophils. T-stack images show the fluorescence recovery over time. Scale bar, 10 μm. Line graph shows the kinetics of bleaching and recovery. n = 15 for JLY front membrane bleaching, n = 11 for JLY side membrane bleaching, n = 12 for JLY back membrane bleaching, and n = 8 for latrunculin B membrane bleaching. Error bars represent SEM.

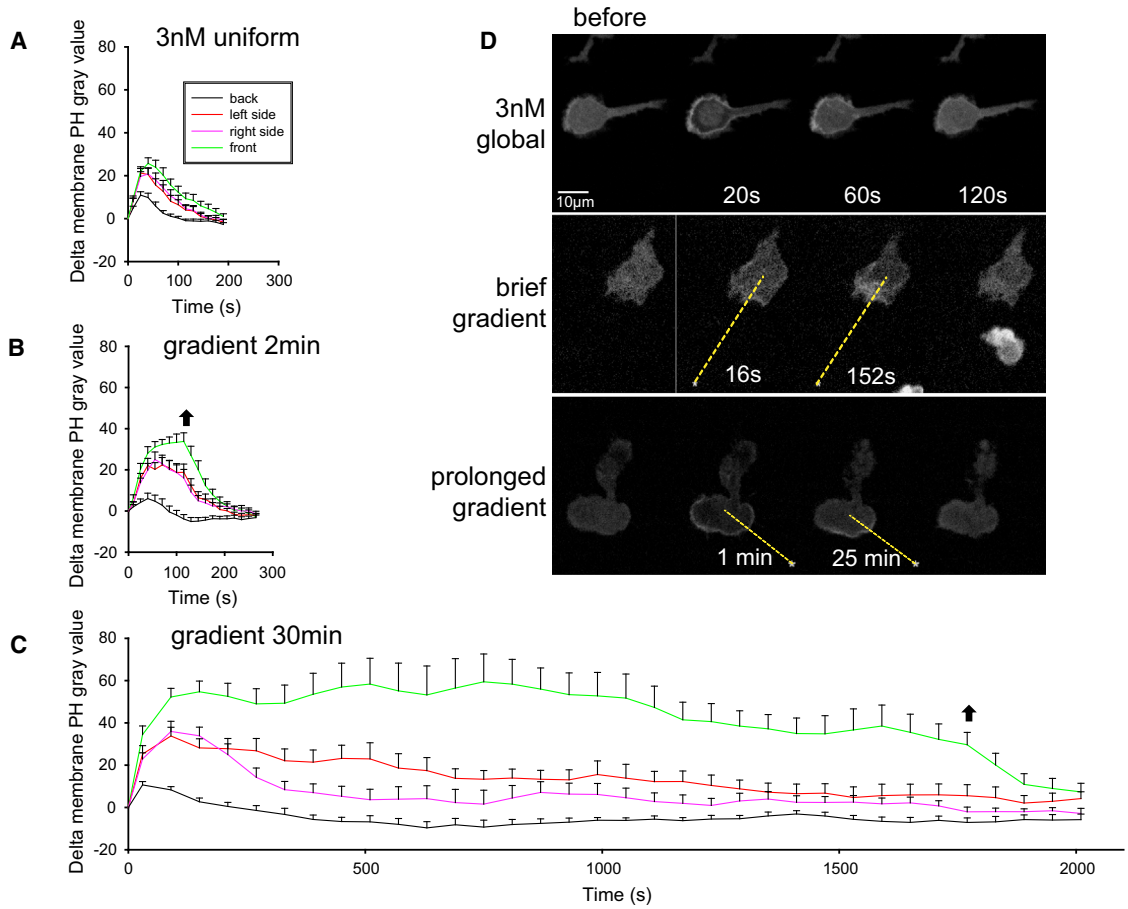

Figure 4. Kinetics and Spatial Distribution of Chemoattractant-Stimulated Responses in JLY-Treated Cells

(A) Kinetics of the response to a persistent uniform stimulus (3 nM fMLP). n = 20. Error bars represent SEM.

(B) Kinetics of the response to a micropipette-generated gradient applied for 2 min (brief gradient). n = 14. Error bars represent SEM.

(C) Kinetics of the response to a micropipette-generated gradient applied for 30 min (prolonged gradient). n = 10. Error bars represent SEM.

(D) Representative fluorescence images of JLY-treated cells expressing PH-AKT from the experiments in (A)–(C). The asterisk shows the location of the micropipette. The dotted yellow line connects the cell centroid to the micropipette tip. Scale bar, 10 μm. See also Movie S8.

cells. Cells were either treated with JLY directly to obtain polarized cells, or first treated with hypotonic buffer to obtain unpolarized cells. With a uniform, low concentration (1 nM) of fMLP, both PH-AKT and Lifeact translocated uniformly to the membrane in cells treated with hypotonic buffer (Figure 5A). Following immobilization of the cytoskeleton with JLY in these rounded cells, PH-AKT still translocated uniformly to the membrane with 1 nM fMLP stimulation. When the immobilized, unpolarized cells were exposed to an fMLP gradient from a micropipette, PH-AKT formed a symmetrical crescent toward the tip. Furthermore, we were able to rapidly and repeatedly reorient the crescent, indicating that the cells had a strong directional response but lacked polarity (Figure 5B; Movie S9).

In contrast, the persistent directional responses of the elongated JLY-treated cells to fMLP gradients were biased toward the axis of polarity. Kymographs show that the PH-AKT signal appeared when the gradient was applied and disappeared when it was removed, whereas the Lifeact signal remained constant throughout the experiment (Figures 5D, 5F, and 5H; Figure S2G; Movie S10). Although the Lifeact signal was consistently more prominent at the morphological front of the cell, some isolated patches of relatively high intensity were also present at the back, contributing to the fluctuations seen in the intensity plots. When the micropipette was placed in front of the cell, PIP_3 accumulation was highest at the front with decreasing responsiveness at the sides and back (Figure 5D). The quantification showed that the response was highest toward the needle and equal on the two sides (Figure 5E). The profile of the distribution of PH-AKT was centered around the needle position and overlapped with the distribution of Lifeact at the front of the cell (Figure 5D). When the pipette was positioned at the side of a cell, the direction of the strongest response was intermediate between a line from the cell's center to the tip of the pipette and the axis of polarity of the cell, as defined by Lifeact. The profiles of the distribution of PH-AKT and Lifeact were shifted (Figure 5F). Consistently, quantification showed that the side toward the needle had a higher response than the opposite side (Figure 5G). Remarkably, when the pipette was positioned at the

back, the steady-state response was at the front (Figures 5H and 5I). The cell continued to respond toward the down side of the gradient until the pipette was lifted (Figure 5H). These observations suggest the responses to the gradient and intrinsic polarity are separable phenomena that are integrated.

DISCUSSION

Our studies of PI3K and SCAR/WAVE activation in moving and immobilized HL-60 neutrophils with uniform increases and gradients of chemoattractant yielded several unexpected and important findings. First, neither cytoskeletal dynamics nor cell movement is required to maintain polarized sensitivity. Second, polarized sensitivity is not dependent on cell shape or volume, membrane curvature or fluidly, or a preexisting distribution of PI3K. It correlates strongly with cytoskeletal architecture. Third, the kinetics of responses to uniform increases and gradients of chemoattractants are the same in unpolarized and polarized cells. Finally, the directional response to the gradient is biased by intrinsic polarity.

Cytoskeletal Dynamics Are Not Needed for Maintenance of Polarity

Figure 6A outlines a putative scheme for the establishment and maintenance of polarity in neutrophils. Chemoattractant fMLP binds to its G protein-coupled receptor (GPCR), releasing $G\beta\gamma$ from inhibitory $G\alpha i$ and activating Ras and PI3K. PIP_3 accumulates locally on the membrane, which activates Rac, leading to actin polymerization and subsequent changes in cytoskeletal architecture. It is generally accepted that feedback regulation from actin to PI3K is through actin polymerization. Consistently, direct photoactivation of Rac, bypassing the GPCR entry point, led to actin polymerization, protrusions, and accumulation of PIP_3. When we separated actin polymerization from actin architecture by treatment with JLY, the accumulation of PIP3 at the leading edge and the activation of PI3K through photoactivation of Rac were reduced. This suggests that feedback activation of PI3K in neutrophils is amplified by new actin polymerization and/or protrusions. However, in cells that had a static F-actin cytoskeleton, both spontaneous and chemoattractant-induced activation of PI3K still occurred and was polarized. To explain these observations, we propose that cytoskeletal architecture itself, not its dynamics, sends a feedback signal that lowers the threshold for activation of the signal transduction network.

Many ideas about polarity have focused on its initial establishment, during which a protrusion is reinforced by positive feedback from signaling or cytoskeletal events and protrusions at other regions are inhibited. Candidates for global inhibition have included depletion of positive regulators, membrane curvature, and membrane tension (Arai et al., 2010; Galic et al., 2012; Houk et al., 2012; Postma and Van Haastert, 2001). However, the studies presented here show that polarized sensitivity can be maintained without cytoskeletal dynamics or cell movement. Once the cells are immobilized, many of the effects of the initial protrusion, such as new surface contact or pressures on the membrane, would be expected to dissipate.

We were able to directly rule out a number of factors as contributors to the maintenance of polarized sensitivity. Sensitivity did not correlate with increased or decreased membrane curvature, nor did sensitivity correspond to regions of weak or strong attachment of the membrane to the cytoskeleton. Membrane fluidity also did not differ between the front and the back. We were unable to measure membrane tension directly, but it seems unlikely that the differential tension of a fluid membrane is maintained in a static cell. We found that PI3K is more easily recruited to regions enriched in static F-actin, which can account for the localized PIP_3 accumulation without invoking effects on PIP_3 degradation. We cannot rule out the possibility that some other upstream signal-transduction components such as a Ras-GEF might be asymmetrically distributed. Further studies are needed to understand how the immobilized cytoskeletal architecture influences the local signal transduction events.

Features of Chemotaxis Are Shared in Dictyostelium and Human Neutrophils

Many pathways involved in chemotaxis are conserved in neutrophils and *Dictyostelium* amoebae (Artemenko et al., 2014; Bagorda et al., 2006; Wang, 2009). Local Ras activation toward chemoattractant and spontaneously at the leading edges of pseudopodia plays a key role in chemotaxis in *Dictyostelium*. In the current study, we show that both K Ras and N Ras are activated by fMLP in neutrophils. Furthermore, by using a longer version of the Ras binding domain of Raf as a biosensor, we were able to study local Ras activation. Like *Dictyostelium*, Ras is activated at the leading edge of migrating HL-60 neutrophils. The temporal and spatial correlation of Ras activation and PIP_3 production suggests they belong to the same signal transduction network, as has been proposed for *Dictyostelium*.

In *Dictyostelium*, separate signal transduction and cytoskeletal networks with different kinetics have been defined. Slower, broader patches and propagating waves of Ras activity and PIP3 production stabilize more rapid fluctuations of the cytoskeleton leading to sustained protrusions and migration (Huang et al., 2013). Spontaneous PIP_3 patches are seen at the basal surface of immobilized neutrophils, suggesting there are similar separate signal transduction and cytoskeletal networks in neutrophils. Although we have not observed propagating waves, the patches have a size and time scale that are consistent with the characteristics of the protrusions. The randomly appearing patches suggest that the signal transduction system is excitable in neutrophils, as has been recently reported for *Dictyostelium* (Arai et al., 2010; Huang et al., 2013). That is, perturbations or noise can drive these events without upstream receptor activation or feedback from downstream cytoskeleton changes. Since the patches are more frequent at the front, the static cytoskeletal architecture appears to bias the excitability, in addition to biasing the response to an external stimulus.

The surprising maintenance of polarized sensitivity in stalled neutrophils we report here has not been described in *Dictyostelium*. Indeed, the fact that *Dictyostelium* cells immobilized with latrunculin lose polarized sensitivity has contributed to the belief that polarity requires cytoskeletal dynamics. It will be interesting to arrest the cytoskeleton of *Dictyostelium* cells with a similar cocktail that preserves morphological polarity and determine whether polarized sensitivity is maintained.

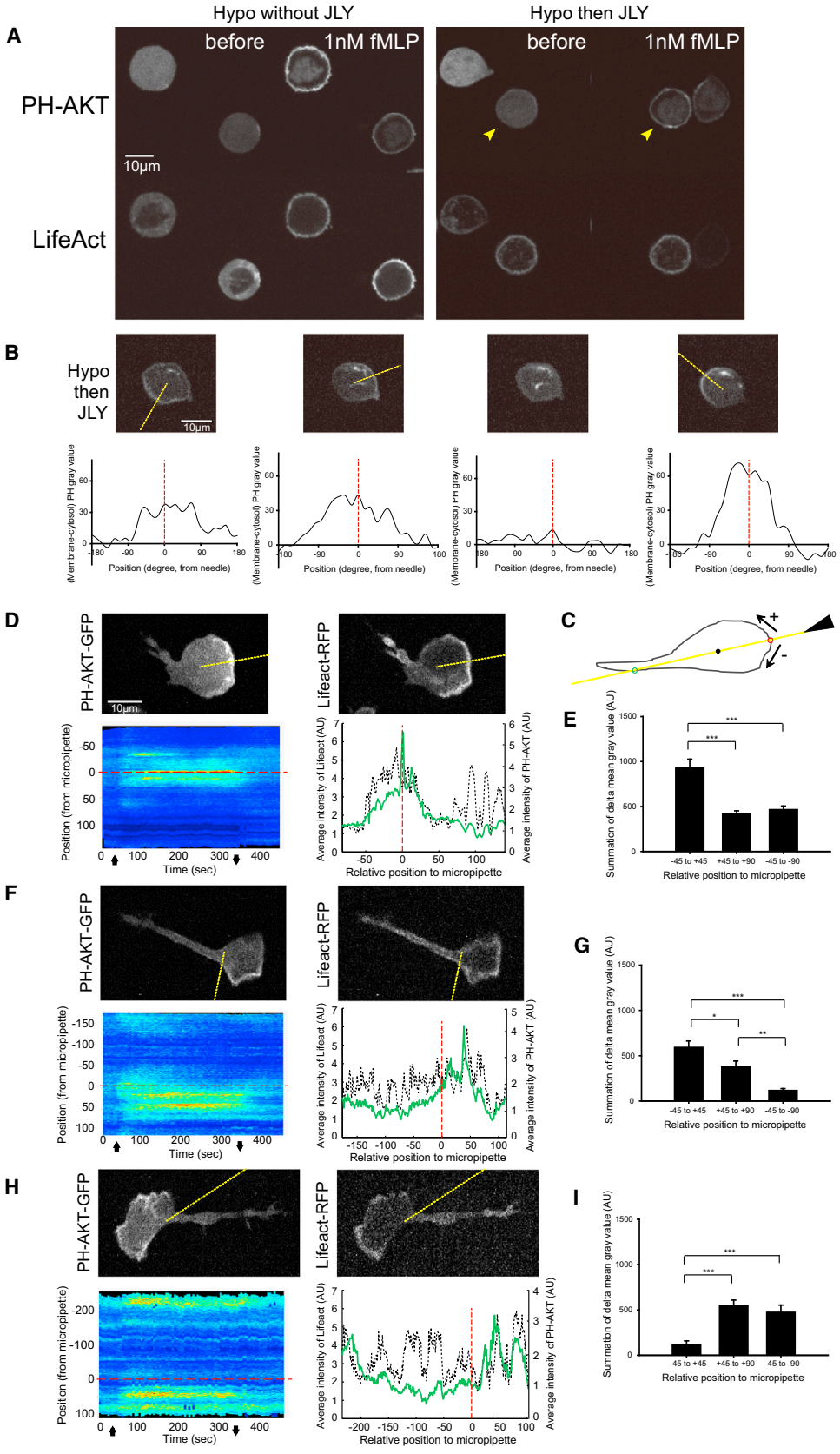

(legend on next page)

Responses to Spatial and Temporal Chemotactic Stimuli Are Retained in JLY-Treated Neutrophils

The stimulus-response behavior in JLY-treated neutrophils, where a uniform global stimulation elicits a transient production of PIP_3 whereas gradient stimulation causes a persistent response, is consistent with the local excitation global-inhibition (LEGI) model (Iglesias and Devreotes, 2012; Levchenko and Iglesias, 2002; Levine et al., 2006; Parent and Devreotes, 1999; Shi et al., 2013; Xiong et al., 2010). This model proposes that the response depends on a balance between local excitatory and global inhibitory processes. Uniform changes in receptor occupancy initiate rapid changes in the excitatory process and slower changes in the inhibitory process, causing a transient response. In a gradient, since inhibition is more global than excitation, there are persistent positive or negative responses at the front and back, respectively.

Our observation of a persistent response in a gradient disagrees with a previous report by Dandekar et al. that PIP_3 accumulation toward a gradient generated by an fMLP-filled micropipette subsided within a few minutes in JLY-treated cells. They argued that receptor resensitization required cytoskeletal dynamics and therefore JLY treatment led to termination of the response (Dandekar et al., 2013). The difference might be due to the steepness of the applied gradient and the time period assessed. We often noted an initial larger response when the gradient was first applied that settled into a persistent steady-state response toward the high side.

Directional Response Depends on the Chemoattractant Gradient and Intrinsic Polarity

The well-known U-turn behavior of neutrophils toward a new source of chemoattractant suggests the influence of intrinsic polarity on directional sensing, but the dynamics make it difficult to distinguish the effects of the gradient and polarity. The ability to stall neutrophils provided a means to study the interaction of the gradient and polarity in isolation. We found that while a persistent steady-state response required a gradient, the response was biased by the intrinsic polarity of the cell. Thus, polarity appears to modulate the threshold for generation of a response. We speculate that the overall directional response of a cell is a combination of the effects of the gradient and intrinsic polarity as shown in Figure 6B. The two vectors in the diagram represent the response to the chemoattractant gradient (C) and the intrinsic polarity (P). In unpolarized cells, the response depends only on C. In polarized cells, however, P causes the overall response to be biased toward the axis of polarity. When the gradient and polarity are aligned, the response to the gradient is enhanced by polarity. With an angle between the vectors, the overall response falls between them. A "vector sum" behavior has been predicted by mathematical calculations of the optimal gradient sensing response by Andrews et al. with the LEGI model (Andrews and Iglesias, 2007). The observation that polarity was able to bias the response even when the gradient was applied close to the back of a cell (Figure 5) can explain why cells can make U-turns when gradients are reversed.

Taken together, these observations suggest that the amplified signal transduction events seen at the leading edge of migrating neutrophils require feedback from actin polymerization and/or cell movement but that a static cytoskeletal architecture is sufficient to differentially affect the threshold for chemoattractant-elicited or noise-generated activity. The anterior-posterior gradient in sensitivity displayed by migrating cells appears to be derived from this altered threshold.

EXPERIMENTAL PROCEDURES

Cell Culture and Virus Infection

HL-60 cells were cultured in RPMI 1640 containing GlutaMAX-1 (GIBCO) supplemented with 20% heat-inactivated fetal bovine serum (Gibco), 100 U/ml penicillin, and 100 mg/ml streptomycin in a 5% CO_2 incubator at 37°C. Differentiation toward neutrophil-like cells was induced by adding 1.3% DMSO (Sigma-Aldrich) into the culture medium for 5 days. HL-60 cells were infected with lentivirus (a gift from Dr. Cooper and Dr. Desiderio) carrying different fluorescent proteins and selected by fluorescence-activated cell sorting (FACS). For a complete description of methods, see Supplemental Experimental Procedures.

Figure 5. Directional Response in Unpolarized and Polarized Cells in a Chemoattractant Gradient

(A) Fluorescence images of neutrophils coexpressing PH-AKT and Lifeact treated with 1:1 hypotonic buffer without (left) or with (right) the addition of JLY and stimulated with fMLP. Arrowheads indicate the PH-AKT signal of the same cell before and 30 s after adding fMLP. Scale bar, 10 μm.

(B) PH-AKT response toward repeatedly reoriented fMLP-filled micropipette in cells treated with hypotonic buffer followed by JLY. Dotted yellow line connects the cell centroid to the pipette tip. Line graphs show the relationship between membrane PH-AKT and chemoattractant gradient direction. Vertical red dotted line is intersection of yellow line in (B) with membrane. Values to the right (or left) were obtained by tracing clockwise (or counterclockwise) to a point on the opposite side of the cell. The pipette was lifted in the third panel. For this condition, the vertical line was kept in the previous position. See also Movie S9.

(C) A schematic of a cell showing how the position from the needle is determined for kymographs in (D), (F), and (H). The red and green circles are the intersections of the cell membrane with the line connecting the micropipette to the cell centroid. The circle closest to the micropipette (red) is defined as "position 0." Values at positions between red and green circles are either positive or negative, as indicated by "+" and "−," respectively.

(D) PH-AKT response to an fMLP-filled micropipette placed toward the front of a JLY-treated cell between 25 and 325 s (marked by the up and down arrows). Snapshots of PH-AKT and Lifeact signals at 200 s are shown. Dotted yellow line as in (B). Kymograph shows the membrane PH-AKT intensity around the entire cell perimeter over time. Intensity plots of the mean intensity of PH-AKT (green line) and Lifeact (dashed line) obtained from ten continuous frames in the middle of the fMLP stimulation are also shown.

(E) Statistics of the response from (D) for 26 separate cells. ***$p < 0.001$. Error bars represent SEM.

(F) PH-AKT response to an fMLP-filled micropipette placed toward the side of JLY-treated cells. Dotted yellow line as in (B). Snapshots, kymographs, and intensity plots as in (D).

(G) Statistics of response from (F) for 20 separate cells. *$p < 0.05$; **$p < 0.01$; ***$p < 0.001$. Error bars represent SEM.

(H) PH-AKT response to an fMLP-filled micropipette placed toward the back of JLY-treated cells. Dotted yellow line as in (B). Snapshots, kymographs, and intensity plots as in (D).

(I) Statistics of response from (H) for 18 separate cells. ***$p < 0.001$. Error bars represent SEM. See also Movie S10 and Figure S2.

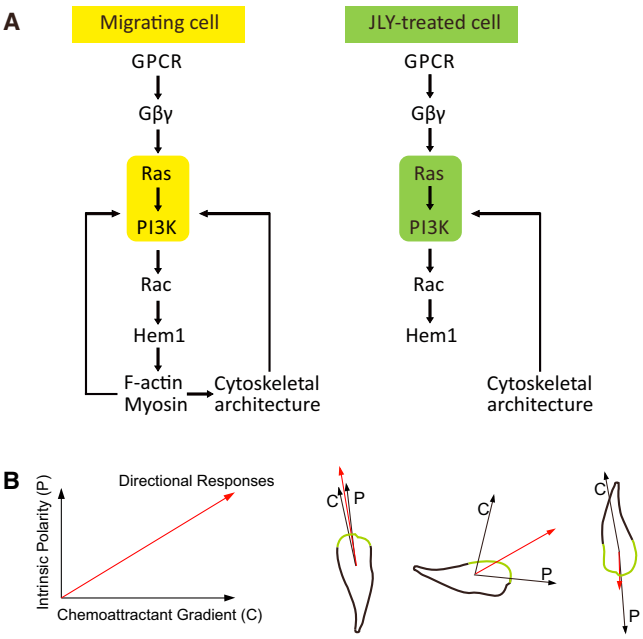

Figure 6. A Putative Scheme for the Establishment and Maintenance of Polarity in Neutrophils

(A) Chemoattractant fMLP binds to its GPCR, thereby releasing Gβγ from inhibitory Gαi and activating Ras and PI3K. PIP_3 accumulates locally on the membrane, which activates Rac, leading to actin polymerization and subsequent changes in cytoskeletal architecture. We propose the feedback regulation of PI3K is dependent on actin polymerization (and weakly from direct interaction with activated Rac). JLY treatment inhibits cytoskeletal dynamics, so Rac-induced actin polymerization is abolished. Cytoskeletal architecture remains and alters the threshold for activation of the signal transduction events by chemoattractant.

(B) Overall directional response of the cell depends on the external chemoattractant gradient and intrinsic polarity. Evidence presented here is consistent with the hypothesis that the overall directional response is a combination of the response to the external gradient and intrinsic polarity as indicated on left. Three examples illustrated cases where the two vectors are almost aligned, nearly orthogonal, or in nearly opposite directions.

Microscopy and Image Analysis

For live-cell imaging, HL-60 neutrophils were collected, washed and resuspended with modified Hank's balanced salt solution (mHBSS) containing 0.2% BSA and then seeded on Lab-Tek chambered cover glasses (NUNC) coated with 50 μg/ml human fibronectin (Sigma-Aldrich). Time-lapse microscopy was performed on a Leica Spinning Disk Confocal microscope. Chemoattractant fMLP (Sigma) was given to cells either globally or delivered by a Femtotips micropipette (Eppendorf). TIRF microscopy was performed using a Nikon Eclipse Ti-E TIRF microscope. FRAP was performed on Zeiss Axiovert 200 laser scanning microscope with the LSM510-Meta confocal module. For immunofluorescent staining, cells were fixed and then stained with anti-PI 3-kinase, p110γ (clone 17D7.2, Merck Millipore) in PBS containing 1% BSA as indicated in Supplemental Experimental Procedures. Images were analyzed with ImageJ (NIH) as described in Supplemental Experimental Procedures.

Different Methods of Generating Immobile Cells

JLY was used to arrest cytoskeletal dynamics and maintain cell shape as described previously (Peng et al., 2011). A total of 10 μM Y27632 was added to neutrophils, and 5 μM latrunculin B and 8 μM jasplakinolide were added 10 min later. In order to get highly polarized cells more easily, for Figures 1B, 3A, 4D, and 5D, 5F, and 5H, the following protocol was used: Y27632 was added for 10 min, then cells were pretreated with 1 nM fMLP for 2 min, before adding jasplakinolide and latrunculin B; after another 10 min, cells were washed with mHBSS to remove fMLP and JLY was added again. PIP_3 production was measured 10 min later. To obtain rounded cells, latrunculin B alone was used for FRAP assays, latrunculin B plus nocodazole was used for global stimulation with fMLP, or hypotonic buffer was used for micropipette assays. In latrunculin B-treated neutrophils, we found that the PH-AKT biosensor tended to aggregate, interfering with the interpretation. Nocodazole inhibited the aggregation. Alternatively, cells were treated with hypotonic buffer (ddH_2O + 1 mM $MgCl_2$ + 1.2 mM $CaCl_2$) for 20 min. Eventually, after fMLP exposure, cells treated with hypotonic buffer would begin to migrate; we added JLY to prevent this.

Photoactivatable Rac Study

HL-60 cells were transfected with yellow fluorescent protein (YFP)-fused photoactivatable Rac1 (a gift from Dr. Yi Wu) and RFP-fused PH-AKT. Cells were irradiated with blue light (Zeiss filter set 38 HE enhanced GFP shift free with the wavelength between 430 nm and 510 nm) for 0.5 s to transiently activate Rac, and images were taken every 10 s using Zeiss fluorescent microscope.

Statistics

Statistical analysis was done using Sigma-plot. Differences among groups were analyzed using one-way ANOVA, followed by Tukey test, if the differences between groups were statistically significant.

SUPPLEMENTAL INFORMATION

Supplemental Information includes Supplemental Experimental Procedures, two figures, and ten movies and can be found with this article online at http://dx.doi.org/10.1016/j.celrep.2014.09.047.

ACKNOWLEDGMENTS

The authors would like to thanks Drs. Christopher Cooper and Stephen Desiderio for the FUW lentivirus packaging system; Dr. Orion D. Weiner for the PH-AKT, C5aR, and Hem-1 constructs; Dr. Yi Wu for the PA-Rac construct; and members of the Devreotes and Iglesias labs for helpful suggestions. This work was supported in part by grants from the NIH (GM 28007 and GM34933 to P.N.D.) and the National Natural Science Foundation of China (81000045 to M.-J.W. and 81000939 to W.-J.C.).

Received: April 10, 2014
Revised: August 29, 2014
Accepted: September 25, 2014
Published: October 23, 2014

REFERENCES

Andrews, B.W., and Iglesias, P.A. (2007). An information-theoretic characterization of the optimal gradient sensing response of cells. PLoS Comput. Biol. *3*, e153.

Arai, Y., Shibata, T., Matsuoka, S., Sato, M.J., Yanagida, T., and Ueda, M. (2010). Self-organization of the phosphatidylinositol lipids signaling system for random cell migration. Proc. Natl. Acad. Sci. USA *107*, 12399–12404.

Artemenko, Y., Lampert, T.J., and Devreotes, P.N. (2014). Moving towards a paradigm: common mechanisms of chemotactic signaling in Dictyostelium and mammalian leukocytes. Cell. Mol. Life Sci. *71*, 3711–3747.

Bagorda, A., Mihaylov, V.A., and Parent, C.A. (2006). Chemotaxis: moving forward and holding on to the past. Thromb. Haemost. *95*, 12–21.

Casella, J.F., Flanagan, M.D., and Lin, S. (1981). Cytochalasin D inhibits actin polymerization and induces depolymerization of actin filaments formed during platelet shape change. Nature *293*, 302–305.

Dandekar, S.N., Park, J.S., Peng, G.E., Onuffer, J.J., Lim, W.A., and Weiner, O.D. (2013). Actin dynamics rapidly reset chemoattractant receptor sensitivity following adaptation in neutrophils. Philos. Trans. R. Soc. Lond. B Biol. Sci. *368*, 20130008.

Frost, A., Unger, V.M., and De Camilli, P. (2009). The BAR domain superfamily: membrane-molding macromolecules. Cell *137*, 191–196.

Funamoto, S., Meili, R., Lee, S., Parry, L., and Firtel, R.A. (2002). Spatial and temporal regulation of 3-phosphoinositides by PI 3-kinase and PTEN mediates chemotaxis. Cell *109*, 611–623.

Futrelle, R.P., Traut, J., and McKee, W.G. (1982). Cell behavior in Dictyostelium discoideum: preaggregation response to localized cyclic AMP pulses. J. Cell Biol. *92*, 807–821.

Galic, M., Jeong, S., Tsai, F.C., Joubert, L.M., Wu, Y.I., Hahn, K.M., Cui, Y., and Meyer, T. (2012). External push and internal pull forces recruit curvature-sensing N-BAR domain proteins to the plasma membrane. Nat. Cell Biol. *14*, 874–881.

Gerisch, G., and Keller, H.U. (1981). Chemotactic reorientation of granulocytes stimulated with micropipettes containing fMet-Leu-Phe. J. Cell Sci. *52*, 1–10.

Gómez-Moutón, C., Lacalle, R.A., Mira, E., Jiménez-Baranda, S., Barber, D.F., Carrera, A.C., Martínez-A, C., and Mañes, S. (2004). Dynamic redistribution of raft domains as an organizing platform for signaling during cell chemotaxis. J. Cell Biol. *164*, 759–768.

Houk, A.R., Jilkine, A., Mejean, C.O., Boltyanskiy, R., Dufresne, E.R., Angenent, S.B., Altschuler, S.J., Wu, L.F., and Weiner, O.D. (2012). Membrane tension maintains cell polarity by confining signals to the leading edge during neutrophil migration. Cell *148*, 175–188.

Howell, A.S., Savage, N.S., Johnson, S.A., Bose, I., Wagner, A.W., Zyla, T.R., Nijhout, H.F., Reed, M.C., Goryachev, A.B., and Lew, D.J. (2009). Singularity in polarization: rewiring yeast cells to make two buds. Cell *139*, 731–743.

Huang, C.H., Tang, M., Shi, C., Iglesias, P.A., and Devreotes, P.N. (2013). An excitable signal integrator couples to an idling cytoskeletal oscillator to drive cell migration. Nat. Cell Biol. *15*, 1307–1316.

Iglesias, P.A., and Devreotes, P.N. (2012). Biased excitable networks: how cells direct motion in response to gradients. Curr. Opin. Cell Biol. *24*, 245–253.

Inoue, T., and Meyer, T. (2008). Synthetic activation of endogenous PI3K and Rac identifies an AND-gate switch for cell polarization and migration. PLoS ONE *3*, e3068.

Levchenko, A., and Iglesias, P.A. (2002). Models of eukaryotic gradient sensing: application to chemotaxis of amoebae and neutrophils. Biophys. J. *82*, 50–63.

Levine, H., Kessler, D.A., and Rappel, W.J. (2006). Directional sensing in eukaryotic chemotaxis: a balanced inactivation model. Proc. Natl. Acad. Sci. USA *103*, 9761–9766.

Meinhardt, H. (1999). Orientation of chemotactic cells and growth cones: models and mechanisms. J. Cell Sci. *112*, 2867–2874.

Neilson, M.P., Veltman, D.M., van Haastert, P.J., Webb, S.D., Mackenzie, J.A., and Insall, R.H. (2011). Chemotaxis: a feedback-based computational model robustly predicts multiple aspects of real cell behaviour. PLoS Biol. *9*, e1000618.

Nishikimi, A., Fukuhara, H., Su, W., Hongu, T., Takasuga, S., Mihara, H., Cao, Q., Sanematsu, F., Kanai, M., Hasegawa, H., et al. (2009). Sequential regulation of DOCK2 dynamics by two phospholipids during neutrophil chemotaxis. Science *324*, 384–387.

Orchard, R.C., Kittisopikul, M., Altschuler, S.J., Wu, L.F., Süel, G.M., and Alto, N.M. (2012). Identification of F-actin as the dynamic hub in a microbial-induced GTPase polarity circuit. Cell *148*, 803–815.

Parent, C.A., and Devreotes, P.N. (1999). A cell's sense of direction. Science *284*, 765–770.

Parent, C.A., Blacklock, B.J., Froehlich, W.M., Murphy, D.B., and Devreotes, P.N. (1998). G protein signaling events are activated at the leading edge of chemotactic cells. Cell *95*, 81–91.

Peng, G.E., Wilson, S.R., and Weiner, O.D. (2011). A pharmacological cocktail for arresting actin dynamics in living cells. Mol. Biol. Cell *22*, 3986–3994.

Postma, M., and Van Haastert, P.J. (2001). A diffusion-translocation model for gradient sensing by chemotactic cells. Biophys. J. *81*, 1314–1323.

Riedl, J., Crevenna, A.H., Kessenbrock, K., Yu, J.H., Neukirchen, D., Bista, M., Bradke, F., Jenne, D., Holak, T.A., Werb, Z., et al. (2008). Lifeact: a versatile marker to visualize F-actin. Nat. Methods *5*, 605–607.

Servant, G., Weiner, O.D., Herzmark, P., Balla, T., Sedat, J.W., and Bourne, H.R. (2000). Polarization of chemoattractant receptor signaling during neutrophil chemotaxis. Science *287*, 1037–1040.

Shi, C., Huang, C.H., Devreotes, P.N., and Iglesias, P.A. (2013). Interaction of motility, directional sensing, and polarity modules recreates the behaviors of chemotaxing cells. PLoS Comput. Biol. *9*, e1003122.

Spector, I., Shochet, N.R., Kashman, Y., and Groweiss, A. (1983). Latrunculins: novel marine toxins that disrupt microfilament organization in cultured cells. Science *219*, 493–495.

Srinivasan, S., Wang, F., Glavas, S., Ott, A., Hofmann, F., Aktories, K., Kalman, D., and Bourne, H.R. (2003). Rac and Cdc42 play distinct roles in regulating PI(3,4,5)P3 and polarity during neutrophil chemotaxis. J. Cell Biol. *160*, 375–385.

Swanson, J.A., and Taylor, D.L. (1982). Local and spatially coordinated movements in Dictyostelium discoideum amoebae during chemotaxis. Cell *28*, 225–232.

Ting-Beall, H.P., Needham, D., and Hochmuth, R.M. (1993). Volume and osmotic properties of human neutrophils. Blood *81*, 2774–2780.

Wang, F. (2009). The signaling mechanisms underlying cell polarity and chemotaxis. Cold Spring Harb. Perspect. Biol. *1*, a002980.

Wang, F., Herzmark, P., Weiner, O.D., Srinivasan, S., Servant, G., and Bourne, H.R. (2002). Lipid products of PI(3)Ks maintain persistent cell polarity and directed motility in neutrophils. Nat. Cell Biol. *4*, 513–518.

Weiner, O.D., Marganski, W.A., Wu, L.F., Altschuler, S.J., and Kirschner, M.W. (2007). An actin-based wave generator organizes cell motility. PLoS Biol. *5*, e221.

Xiong, Y., Huang, C.H., Iglesias, P.A., and Devreotes, P.N. (2010). Cells navigate with a local-excitation, global-inhibition-biased excitable network. Proc. Natl. Acad. Sci. USA *107*, 17079–17086.

Xu, J., Wang, F., Van Keymeulen, A., Herzmark, P., Straight, A., Kelly, K., Takuwa, Y., Sugimoto, N., Mitchison, T., and Bourne, H.R. (2003). Divergent signals and cytoskeletal assemblies regulate self-organizing polarity in neutrophils. Cell *114*, 201–214.

Zheng, L., Eckerdal, J., Dimitrijevic, I., and Andersson, T. (1997). Chemotactic peptide-induced activation of Ras in human neutrophils is associated with inhibition of p120-GAP activity. J. Biol. Chem. *272*, 23448–23454.